Journal of Theoretical and Applied Mechanics, Sofia, Vol.54 (2024) pp. 278-291
SOLID MECHANICS

TIME-DEPENDENT DELAMINATION OF MULTILAYERED INHOMOGENEOUS BEAM LOADED IN PURE TORSION: AN ANALYTICAL SOLUTION

V. RIZOV*

Department of Technical Mechanics,
University of Architecture, Civil Engineering and Geodesy,
1 Chr. Smirnensky blvd., 1046 – Sofia Bulgaria

[Received: 14 June 2023. Accepted: 1 October 2024]

doi: https://doi.org/10.55787/jtams.24.54.3.278

ABSTRACT: The multilayered inhomogeneous beam configuration considered in this paper exhibits delamination fracture that is time-dependent due to the viscoelastic behaviour. Besides, the two external torsion moments applied on the beam vary smoothly with time. The beam has a rectangular cross-section. The layers of the beam are continuously inhomogeneous in longitudinal direction. The two crack arms are loaded in pure torsion. A solution of the strain energy release rate for the delamination is derived by analyzing the time-dependent strain energy stored in the beam structure. An alternative method based on the analysis of the beam compliances under the two torsion moments is applied in order to verify the solution of the strain energy release rate.

KEY WORDS: multilayered beam, time-dependent delamination, torsion, viscoelastic behaviour, analytical approach

1 INTRODUCTION

In recent decades, there has been an increased interest in the development and application of inhomogeneous structural materials. The functionally graded materials are an important type of continuously inhomogeneous materials whose properties vary smoothly along one or more spatial coordinates in the structural component [1–3]. The variation of microstructure and material properties can be tailored during manufacturing of the functionally graded structural member. In this way, continuously inhomogeneous (functionally graded) materials with superior

properties are manufactured which makes them irreplaceable in aeronautics, nuclear reactors and microelectronics.

A number of investigations have been devoted to the continuously inhomogeneous materials [4–7]. The purpose of these investigations has been mainly to contribute to

*Corresponding author e-mail: v_rizov_fhe@uacg.bg

the development of the technologies of functionally graded materials and to broaden the area of their application in modern engineering.

One of the factors influencing the proper functioning of engineering structures made of continuously inhomogeneous (functionally graded) materials is the fracture behaviour [8–12]. Cracks and their effect on strength of continuously inhomogeneous load-carrying constructions are thoroughly analyzed in [8]. A method for assessing the effect of cracks is developed and applied for rectangular plates loaded in tension and beam structures subjected to bending [8]. Useful analyses of the mechanical behaviour of functionally graded beam constructions with edge cracks are developed in [9]. The beams under consideration in [9] are loaded in bending. A parametric investigation is carried-out to show the effects of the location and number of cracks on buckling characteristics of the beams. The influence of boundary conditions is also evaluated [9]. Various fracture studies of composite materials and structures with graded composition are presented in [10]. The influence of microstructural gradation of the material on the behaviour of cracks is discussed and assessed. Besides for static loading, fracture is analyzed also under fatigue crack loading conditions. It should be mentioned that the fracture studies reviewed in [10] deal in the main with structural members and components subjected to tension. Functionally graded engineering beam constructions with a single delamination are analyzed in [11]. Analytical solutions for delaminated beams loaded in bending are derived. The influence of the variation of material properties along the beam thickness on the delamination is clarified. The effects of delamination length and location are also studied [11]. Cracked functionally graded beams are explored analytically in [12]. A method that uses an equivalent homogeneous beam structure of variable thickness for the cracked beam is developed and successfully applied. Different variations of the modulus of elasticity along the beam span are considered for a functionally graded beam on two supports subjected to bending by a vertical force [12].

A type of inhomogeneous material which is very suitable for use in various lightweight structural applications is the multilayered inhomogeneous material made of adhesively bonded layers of different inhomogeneous materials. It is clear that keeping the bonding at the interfaces between layers intact is of vital importance for the structural integrity and reliability of multilayered beam members [13–20]. The separation of beam layers known as delamination fracture in many cases represents a major cause for catastrophic failure of multilayered load-bearing engineering structures. This is due mainly to the fact that strength and stiffness of each delaminated area of a multilayered structural member are significantly lower in comparison with these of intact parts of the structure. Delamination leads also to reduction of the load-carrying capacity and has a heavy negative impact on overall working, safety and durability of the structural system. Prevention of delamination of multilayered systems generally

requires analysis of various aspects of delamination fracture and assessment of a big number of factors and parameters which influence the delamination behaviour.

Delaminated multilayered linear-elastic beam structures subjected to four-point bending are investigated analytically in [20]. A solution in closed form for the strain energy release rate is derived. Different layered systems are considered and discussed. The delamination fracture analysis reveals the most important dependences of the strain energy release rate on factors like the beam aspect ratio, the number and thickness of layers, the ratio of the modulus of elasticity and the location of the delamination crack along the thickness of the beam [20]. Functionally graded beam structural members with a delamination crack are thoroughly analyzed in [21]. The delaminated beams that are under consideration are loaded in static bending [21]. The buckling behaviour of functionally graded beams with delaminated layers is studied in [22]. A general formula for determination of the critical buckling force in non-dimensional form is derived [22]. Various analytical solutions for beam and plate load-carrying structures with delamination cracks subjected to bending are presented in [23]. Determination of the strain energy release rate is discussed in detail. An approach for calculating of the strain energy release rate in delaminated quasi-homogeneous beam configurations exhibiting linear-elastic behaviour is worked-out [23].

The above literature survey clearly indicates that analyses of delamination behaviour of different beam engineering structures and components have been concerned predominantly with beams loaded in bending. However, multilayered beams loaded in pure torsion are frequently used as structural components of various constructions. For recent years, studies of delamination of multilayered inhomogeneous load-carrying systems loaded in torsion have been focussed on beam structures of circular cross-section [24,25], although multilayered beams of rectangular cross-section are more widely applied in structural engineering.

Therefore, the aim of this paper is to analyze the delamination in a multilayered beam structure of rectangular cross-section under pure torsion. The emphasis is put on the time-dependent delamination since in many cases the structures exhibit viscoelastic behaviour. Besides, the beam considered in this paper is under two external torsion moments which vary continuously with time. A solution of the strain energy release rate is derived. The solution is verified by analyzing the beam compliances. The solution is applied to perform a parametric investigation.

2 Time-Dependent Delamination Analysis under Torsion

The multilayered viscoelastic beam displayed in Fig. 1 has a rectangular cross-section of width, b, and thickness, h. The length of the beam is l. The beam is clamped in its right-hand end. There is a delamination crack in the beam (Fig. 1). The length of the

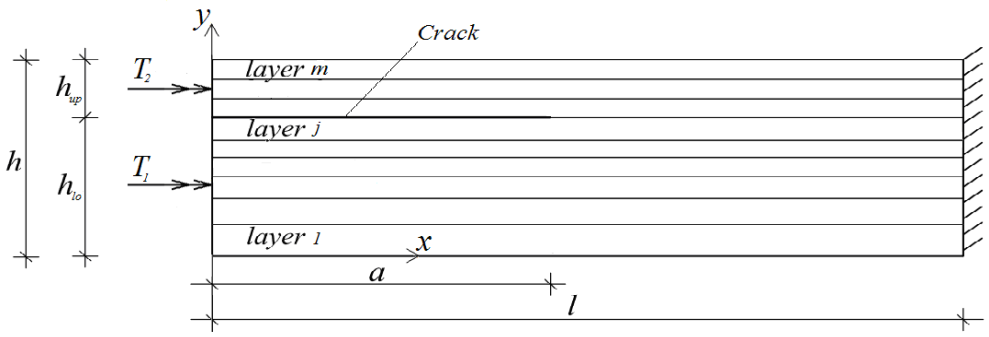

Fig. 1: Multilayered inhomogeneous viscoelastic beam structure with delamination loaded in pure torsion.

delamination is a. The thickness of the lower and upper crack arm are h_{lo} and h_{up}, respectively. The beam is loaded by two torsion moments, T_1 and T_2 applied at the free ends of the lower and upper crack arm, respectively. The variation of the torsion moments with time, t, is expressed as

$$T_1 = v_1 t\,, \tag{1}$$

$$T_2 = v_2 t\,, \tag{2}$$

where v_1 and v_2 are parameters governing the variation of the torsion moments.

The mechanical behaviour of the j-th layer of the beam is modelled by the linear viscoelastic model displayed in Fig. 2. The model is under shear stress, τ_j, that varies with time according to the following expression:

$$\tau_j = v_{\tau_j} t\,, \tag{3}$$

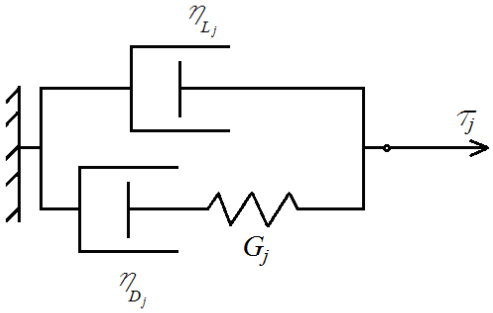

Fig. 2: Viscoelastic mechanical model.

where the parameter v_{τ_j} governs the variation of the shear stress. By analyzing the equilibrium of the components of the viscoelastic model, one derives the following constitutive law

$$\gamma_j = \frac{v_{\tau_j}}{\theta_j^2}\Big(\frac{1}{\eta_{L_j}} - \frac{\beta_j}{\theta_j}\Big)(\mathrm{e}^{-\theta_j t} - 1) + \frac{\beta_j v_{\tau_j}}{2\theta_j} t^2 + \frac{v_{\tau_j}}{\theta_j}\Big(\frac{1}{\eta_{L_J}} - \frac{\beta_J}{\theta_j}\Big), \tag{4}$$

where

$$\theta_j = \frac{G_j}{\eta_{L_j}}\Big(1 + \frac{\eta_{L_j}}{\eta_{D_j}}\Big), \tag{5}$$

$$\beta_j = \frac{G_j}{\eta_{D_j}\eta_{L_j}}\,. \tag{6}$$

In formulae (4), (5) and (6), γ is the shear strain, G_j is the shear modulus of the spring, η_{D_j} and η_{L_j} are the coefficients of viscosity of the dashpots (Fig. 2).

The time-dependent shear modulus, $G_{*\,j}$, of the viscoelastic model is found as

$$G_{*\,j} = \frac{\tau_j}{\gamma_j}\,, \tag{7}$$

where $j = 1, 2, \ldots, m$ (m is the number of layers in the beam). By combining of (3), (4) and (7), one obtains

$$G_{*j} = \Big[\frac{1}{\theta_j^2 t}\Big(\frac{1}{\eta_{L_j}} - \frac{\beta_j}{\theta_j}\Big)(\mathrm{e}^{-\theta_j t} - 1) + \frac{\beta_j}{2\theta_j} t + \frac{1}{\theta_j}\Big(\frac{1}{\eta_{L_j}} - \frac{\beta_j}{\theta_j}\Big)\Big]^{-1}. \tag{8}$$

The beam is continuously inhomogeneous along its length. The distributions of the shear modulus and the coefficients of viscosity of the j-th layer of the beam in longitudinal direction are written as

$$G_j = G_{B_j} + \frac{G_{H_j} - G_{B_j}}{l^{\omega_j}} x^{\omega_j}\,, \tag{9}$$

$$\eta_{D_j} = \eta_{DB_j} + \frac{\eta_{DH_j} - \eta_{DB_j}}{l^{\rho_j}} x^{\rho_j}\,, \tag{10}$$

$$\eta_{L_j} = \eta_{LB_j} + \frac{\eta_{LH_j} - \eta_{LB_j}}{l^{\mu_j}} x^{\mu_j}\,, \tag{11}$$

where G_{B_j}, η_{DB_j} and η_{LB_j} are the values of G_j, η_{D_j} and η_{L_j} at the free end of the beam. The abscise x in (9), (10) and (11) varies in the interval $[0; l]$. The values of G_j, η_{D_j} and η_{L_j} at the right-hand end of the beam are denoted by G_{H_j}, η_{DH_j} and η_{LH_j}, respectively. The parameters, ω_j, ρ_j and μ_j, govern the variation of G_j, η_{D_j} and η_{L_j}, respectively.

The strain energy release rate, G, for the delamintion in Fig. 1 is derived by using the following dependency:

$$G = \frac{\mathrm{d}U}{b\mathrm{d}a}\,, \tag{12}$$

where the stain energy, U, in the beam is found as

$$U = \sum_{i=1}^{i=m_1} \int_0^a \Big(\iint\limits_{(A_j)} u_{01j}\mathrm{d}A \Big)\mathrm{d}x + \sum_{i=1}^{i=m_2} \int_0^a \Big(\iint\limits_{(A_j)} u_{02j}\mathrm{d}A \Big)\mathrm{d}x + \sum_{i=1}^{i=m} \int_a^{l-a} \Big(\iint\limits_{(A_j)} u_{03j}\mathrm{d}A \Big)\mathrm{d}x\,, \tag{13}$$

where m_1 and m_2 are numbers of layers in the lower and upper crack arm, A_j is the area of the cross-section of the j-th layer, u_{01j}, u_{02j} and u_{03j} are the strain energy densities in the j-th layer of the lower and the upper crack arm and the un-cracked beam portion, $a \leq x \leq l$.

The strain energy density, u_{01j}, is written as

$$u_{01j} = \frac{\tau_j^2}{2G_{*_j}}\,, \tag{14}$$

where the shear stress, τ_j, in the j-th layer of the lower crack arm is found by using the following formula for shear stress in a multilayered beam under torsion [26]:

$$\tau_j = \frac{T_1}{S_1}\Bigg\{ \Big[\sum_{k=1,3,\ldots}^{\infty} (P_{k,j}\cosh\alpha_k y + Q_{k,j}\sinh\alpha_k y)\alpha_k \sin\alpha_k z \Big]^2 + \Big[\sum_{k=1,3,\ldots}^{\infty} \Big(P_{k,j}\sinh\alpha_k y + Q_{k,j}\cosh\alpha_k y + \frac{8G_{*_j}b^2}{k^3\pi^3} \Big)\alpha_k \cos\alpha_k z \Big]^2 \Bigg\}^{\frac{1}{2}}. \tag{15}$$

The axes, y and z, are shown in Fig. 3. The quantity, α_k, is determined as [26]

$$\alpha = \frac{k\pi}{b}\,. \tag{16}$$

The following recurrent expressions are used to obtain the quantities $P_{k,j}$ and $Q_{k,j}$ [26]:

$$P_{k,j} = \frac{2}{(g_{j,j+1}-1)\sinh 2\alpha_k h_j}\Big[Q_{k,j+1}g_{j,j+1} + \tag{17}$$

$$+ Q_{k,j}(\sinh^2 \alpha_k h_j - g_{j,j+1} \cosh^2 \alpha_k h_j)$$
$$+ g_{j,j+1}(r_{k,j+1} - r_{k,j}) \cosh \alpha_k h_j)\Big],$$

(18) $$P_{k,j+1} = \frac{2}{(g_{j,j+1} - 1) \sinh 2\alpha_k h_j}\Big[Q_{k,j+1}(\cosh^2 \alpha_k h_j - g_{j,j+1} \sinh^2 \alpha_k h_j)$$
$$- Q_{k,j} + (r_{k,j+1} - r_{k,j}) \cosh \alpha_k h_j)\Big],$$

(19)

where

(20) $$g_{j,j+1} = \frac{G_* j}{G_{*(j+1)}},$$

(21) $$r_{k,j} = \frac{8 G_{*j} b^2}{k^3 \pi^3}.$$

Here, $j = 1, 2, \ldots, m_1 - 1$. The quantities, h_j, are defined in Fig. 3. Besides [26],

(22) $$P_{k,1} = -\frac{Q_{k,1} \cosh \alpha_k h_0 + r_{k,1}}{\sinh \alpha_k h_0},$$

(23) $$P_{k,n} = -\frac{Q_{k,n} \cosh \alpha_k h_n + r_{k,n}}{\sinh \alpha_k h_n}.$$

All unknowns, $P_{k,j}$ and $Q_{k,j}$, with the same index, k, can be determined consecutively by equations (17), (18), (22) and (24).

The stiffness in torsion, S_1, of the lower crack arm involved in (15) is found as [26]

(24) $$S_1 = \frac{8}{\pi^2} \sum_{k=1,3,\ldots}^{\infty} \frac{1}{k^2}\Big\{\frac{\alpha_k}{2} \sum_{j=1}^{m_1} r_{k,j}(h_j - h_{j-1})$$
$$+ \sum_{j+1}^{m_1} P_{k,j} \sinh \frac{\alpha_k (h_j + h_{j-1})}{2} \sinh \frac{\alpha_k (h_j - h_{j-1})}{2}$$
$$+ \sum_{j+1}^{m_1} Q_{k,j} \sinh \frac{\alpha_k (h_j - h_{j-1})}{2} \cosh \frac{\alpha_k (h_j + h_{j-1})}{2}\Big\}$$

Formula (14) is applied also to calculate u_{02_j}. For this purpose, m_1, T_1 and S_1 are replaced with m_2, T_2 and S_2, where S_2 is the stiffness in torsion of the upper crack arm. The strain energy density, u_{03_j}, is found be replacing of m_1, T_1 and S_1 with m, $T_1 + T_2$ and S_3 in (14) (S_3 is the stiffness in torsion of the un-cracked beam portion).

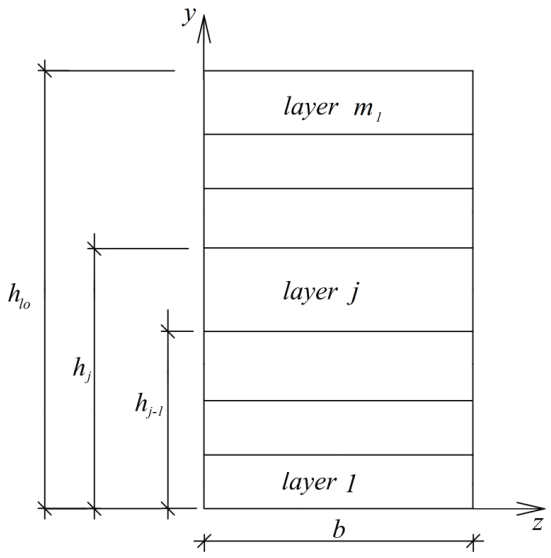

Fig. 3: Cross-section of the lower crack arm.

Formula (24) is applied to obtain S_2 and S_3. For this purpose, m_1 is replaced with m_2 and m.

By combining (12) and (13), one derives

(25)
$$G = \frac{1}{b}\Big[\sum_{i=1}^{i=m_1}\Big(\iint_{(A_j)} u_{01j}\mathrm{d}A\Big)+\sum_{i=1}^{i=m_2}\Big(\iint_{(A_j)} u_{02j}\mathrm{d}A\Big)-\sum_{i=1}^{i=m}\Big(\iint_{(A_j)} u_{03j}\mathrm{d}A\Big)\Big],$$

where the strain energy densities are determined at $x = a$. The integration in (25) is performed by MatLab computer program. Formula (25) is applied to calculate the strain energy release rate at various values of time.

In order to verify (25), an alternative method for obtaining of the strain energy release rate based on analysis of the beam compliances, C_1 and C_2, is used. The compliances are written as

(26)
$$C_1 = \frac{\varphi_1}{T_1}, \qquad C_2 = \frac{\varphi_2}{T_2},$$

where φ_1 and φ_2 are the angles of twist of the free ends of the lower and crack arms, respectively. The following expressions for φ_1 and φ_2 are obtained by applying the integrals of Maxwell-Mohr:

(27)
$$\varphi_1 = \int_0^a \frac{T_1}{S_1}\mathrm{d}x + \int_a^t \frac{T_1+T_2}{S_3}\mathrm{d}x,$$

$$\varphi_2 = \int_0^a \frac{T_2}{S_2}\mathrm{d}x + \int_a^t \frac{T_1 + T_2}{S_3}\mathrm{d}x\,. \tag{28}$$

By using the compliances, the strain energy release rate is found as

$$G = \frac{T_1^2}{2b}\frac{dC_1}{da_1} + \frac{T_2^2}{2b}\frac{dC_2}{da_1}\,. \tag{29}$$

The strain energy release rates determined by applying (29) are identical to these obtained by (25) which is a conformation of the correctness of the present analysis.

3 Parametric Investigation

A parametric investigation is carried-out by applying the solution of the strain energy release rate derived in this paper. For this purpose, the following data are used: $b = 0.015$ m, $h = 0.020$ m, $l = 0.200$ m, $\omega_j = 0.7$, $\rho_j = 0.8$, $\mu_j = 0.9$, $m = 3$, $m_1 = 2$, $v_1 = 0.6 \times 10^{-7}$ Nm/s and $v_2 = 0.6 \times 10^{-7}$ Nm/s.

One can examine the evolution of the strain energy release rate with time in Fig. 4. It should be specified that the strain energy release rate and time in Fig. 4 are presented in non-dimensional form by using the following dependences: $G_N = G/(G_{B_1} b)$ and $t_N = tG_{B_1}/\eta_{DB_1}$. Besides, the strain energy release rate in Fig. 4 is obtained for three values of parameter, v_1. It can be observed in Fig. 4 that when v_1 increases, the strain energy release rate also increases.

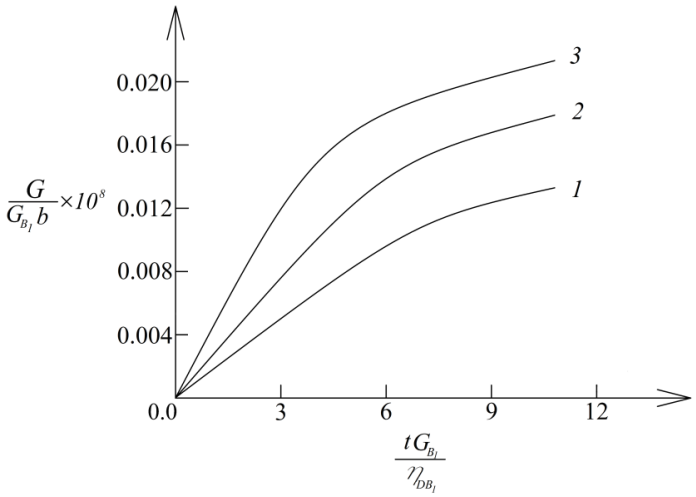

Fig. 4: The strain energy release rate presented as a function of time (curve 1 – at $v = 0.2 \times 10^{-7}$ Nm/s, curve 2 – at $v = 0.4 \times 10^{-7}$ Nm/s and curve 3 – at $v = 0.6 \times 10^{-7}$ Nm/s).

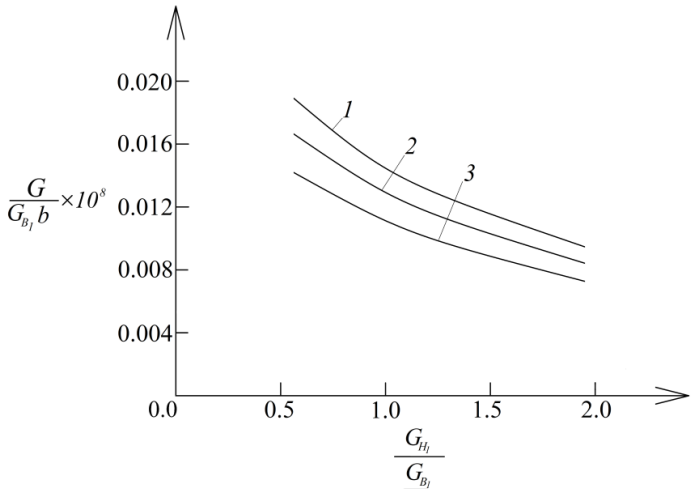

Fig. 5: The strain energy release rate presented as a function of G_{H_1}/G_{B_1} ratio (curve 1 – at $\eta_{DH_1}/\eta_{DB_1} = 0.5$, curve 2 – at $\eta_{DH_1}/\eta_{DB_1} = 1.0$ and curve 3 – at $\eta_{DH_1}/\eta_{DB_1} = 2.0$).

The effects of G_{H_1}/G_{B_1} and η_{DH_1}/η_{DB_1} ratios on the strain energy release rate is investigated (these ratios characterize the change of G_1 and η_{D_1} in layer 1 along the length of the beam). The results of the investigation are depicted in Fig. 5. The inspection of the curves in Fig. 5 reveals that the strain energy release rate reduces when G_{H_1}/G_{B_1} increases. The effect of η_{DH_1}/η_{DB_1} ratio is similar (increase of η_{DH_1}/η_{DB_1} ratio induces reduction of the strain energy release rate (Fig. 5)).

The influence of η_{LH_1}/η_{LB_1} and a/l ratios on the strain energy release rate is investigated too. The ratios, η_{LH_1}/η_{LB_1} and a/l, characterize the variation of the coefficient of viscosity, η_{L_1}, in longitudinal direction of layer 1 and the length of the crack, respectively. The strain energy release rate is presented as a function of η_{LH_1}/η_{LB_1} ratio at three a/l ratios in Fig. 6. It is evident form Fig. 6 that increase of η_{LH_1}/η_{LB_1} ratio leads to reduction of the strain energy release rate. The increase of a/l ratio causes also reduction of the strain energy release rate (Fig. 6).

An analysis of the effect of the ratio of the coefficients of viscosity in layer 1 and layer 2 of the beam on the strain energy release rate is carried-out. The results of this analysis are illustrated in Fig. 7 when the strain energy release rate is presented as a function of η_{LB_2}/η_{LB_1} ratio for three h/b ratios. The curves in Fig. 7 indicate that increase of η_{LB_2}/η_{LB_1} ratio induces reduction of the strain energy release rate. One can observe in Fig. 7 that the strain energy release rate decreases substantially when h/b ratio increases.

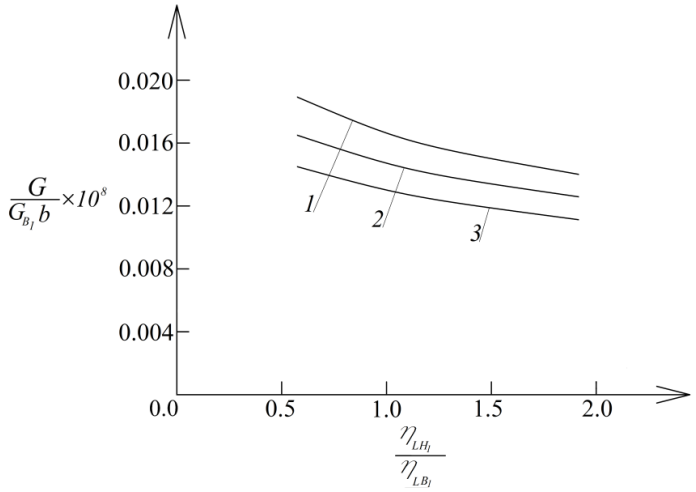

Fig. 6: The strain energy release rate presented as a function of η_{LH_1}/η_{LB_1} ratio (curve 1 – at $a/l = 0.3$, curve 2 – at $a/l = 0.6$ and curve 3 – at $a/l = 0.9$).

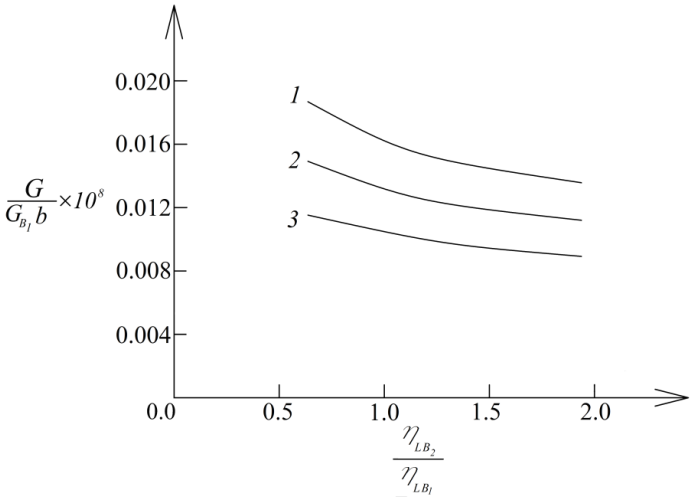

Fig. 7: The strain energy release rate presented as a function of η_{LB_2}/η_{LB_1} ratio (curve 1 – at $h/b = 1.333$, curve 2 – at $h/b = 1.666$ and curve 3 – at $h/b = 2.000$).

The effect of the ratio of shear moduli of layers 1 and 3 on the strain energy release rate is visualised in Fig. 8. It can be observed in Fig. 8 that the strain energy release rate reduces with increasing of G_{B_3}/G_{B_1} and G_{H_3}/G_{B_3} ratios.

A verification of the analytical solution derived in this paper is carried-out also

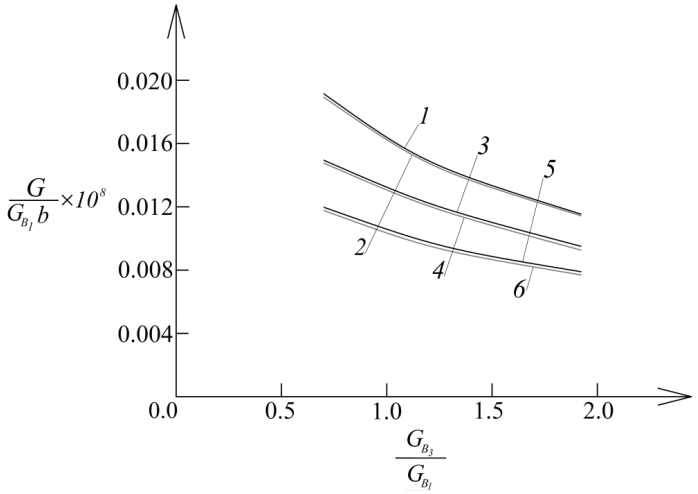

Fig. 8: The strain energy release rate presented as a function of $G_{B_3}/G + B_1$ ratio at $G_{H_3}/G_{B_3} = 0.5$ (curve 1 – analytical solution, curve 2 – numerical analysis), $G_{H_3}/G_{B_3} = 1.0$ (curve 3 – analytical solution, curve 4 – numerical analysis) and $G_{H_3}/G_{B_3} = 2.0$ (curve 5 – analytical solution, curve 6 – numerical analysis).

by performing numerical analysis by using the ANSYS package. The strain energy release rate for the delamination is determined numerically by applying the method of the virtual crack closure [27]. For this purpose, the beam under consideration is modelled by using the 3-D mesh developed in [28]. The results for the strain energy release rate obtained by the numerical analysis are shown in Fig. 8 for comparison with results of the analytical solution. The curves in Fig. 8 indicate a good correspondence between the analytical solution and the numerical analysis.

4 Conclusions

Analysis of the time-dependent delamination in a multilayered inhomogeneous beam structure of rectangular cross-section loaded in pure torsion is developed. The beam has viscoelastic behaviour. The two external torsion moments applied on the beam vary smoothly with time. A solution of the strain energy release rate is derived by using the time-dependent strain energy. The compliances of the beam under torsion are analyzed in order to verify the solution obtained. The parametric investigation performed indicates that the strain energy release rate reduces when G_{H_1}/G_{B_1}, η_{DH_1}/η_{DB_1}, η_{LH_1}/η_{LB_1}, η_{LB_2}/η_{LB_1}, G_{B_3}/G_{B_1} and G_{H_3}/G_{B_3} ratios increase. It is found also that the increase of h/b ratio causes a substantial reduction of the strain energy release rate (this finding is explained with the increase of the beam stiffness

induced by the increase of h/b ratio). The analysis reveals that the strain energy release rate is very sensitive with respect to the value of the parameter, v_1, that governs the variation of the external loading. It is found that when the parameter, v_1, increases, the strain energy release rate increases too.

REFERENCES

[1] M. GASIK (2010) Functionally graded materials: bulk processing techniques. *International Journal of Materials and Product Technology* **39** 20-29.

[2] G. UDUPA, S. SHRIKANTHA RAO, K. RAO GANGADHARAN (2014) Functionally Graded Composite Materials: An Overview. *Procedia Materals Science* **5** 1291-1299.

[3] S. BOHIDAR, R. SHARMA, P. MISHRA (2014) Functionally graded materials: A critical review. *International Journal of Research* **1** 289-301.

[4] M. EL-WAZERY, A. EL-DESOUKY (2015) A review on functionally graded ceramic-metal materials. *Material Environment Science* **6** 1369-1376.

[5] M. NAEBE, K. SHORVANIMOGHADDAM (2016) Functionally graded materials: A review of fabrication and properties. *Applied materials today* **5** 223-245.

[6] R. MAHAMOOD, E. AKINLABI (2017) "Functionally Graded Materials". Springer.

[7] A. BAKSA (2020) Saint-Venant torsion of a functionally graded circular bar with a radial slit. *Journal of Theoretical and Applied Mechanics* **50** 083-101.

[8] A. CARPINTERI, N. PUGNO (2006) Cracks in re-entrant corners in functionally graded materials. *Engineering Fracture Mechanics* **73** 1279-1291.

[9] J. YANG, Y. CHEN (2008) Free vibration and buckling analyses of functionally graded beams with edge cracks. *Composite Structues* **83** 48-60.

[10] M.T. TILBROOK, R.J. MOON, M. HOFFMAN (2005) Crack propagation in graded composites. *Composites Science and Technology* **65** 201-220.

[11] Y. LIU, J. XIAO, D. SHU (2014) Free vibration of exponentially graded beams with single delamination. *Procedia Engineering* **75** 164-168.

[12] A.K. UPADHYAY, K.R.Y. SIMHA (2007) Equivalent homogeneous variable depth beams for cracked FGM beams: compliance approach. *International Journal of Fracture* **144** 209-213.

[13] I. MARKOV, D. DINEV (2005) Theoretical and experimental investigation of a beam strengthened by bonded composite strip. *Reports of International Scientific Conference* VSU'2005.

[14] J.S. KIM, K.W. PAIK, S.H. OH (1999) The Multilayer-Modified Stoney's Formula for Laminated Polymer Composites on a Silicon Substrate. *Journal of Applied Physics* **86** 5474-5479.

[15] M. FINOT, S. SURESH (1996) Small and large deformation of thick and thin-film multilayers: effect of layer geometry and compositonal gradients. *Journal of the Mechanics and Physics of Solids* **44** 683-721.

[16] G. STAVROULAKIS, P. PANAGIOTOPOULOS (1991) Delaminafion of Multilayered Plates in Bending under Monotone Boundary and Non- monotone Interlayer Conditions. A Variational-Hemivariational Inequality Approach. *Journal of Theoretical and Applied Mechanics* **22** 038-046.

[17] V. RIZOV (2018) Analytical study of elastic-plastic fracture in the crack-lap shear multilayered beam configuration. *Journal of Theoretical and Applied Mechanics* **48** 061-077.

[18] V. RIZOV, H. ALTENBACH (2020) Influence of material non-linearity on delamination in multilayered three-point bending beams. *Journal of Theoretical and Applied Mechanics*. **50** 070-082.

[19] V. RIZOV, H. ALTENBACH (2023) Delamination of multilayered beams with non-linear viscoelastic behaviour under strains of step-like varying velocity. *Journal of Theoretical and Applied Mechanics* **53** 099-115.

[20] C.H. HSUEH, W.H. TUAN, W.C.J. WEI (2009) Analyses of steady-state interface fracture of elastic multilayered beams under four-point bending. *Scripta Materialia* **60** 721-724.

[21] V. BIRMAN, W. BYRD (2006) Functionally graded stitched laminates: illustration on an example of a double cantilever beam. *Journal of Aerospace Engineering* **19** 893-911.

[22] M.E. TORKI, J.N. REDDY (2016) Buckling of functionally-graded beams with partially delaminated piezoelectric layers. *International Journal of Structural Stability and Dynamics* **16** 145-170.

[23] J.W. HUTCHISON, Z. SUO (1992) Mixed mode cracking in layered materials. *Advances in Applied Mechanics* **64** 804-810.

[24] V. RIZOV (2018) Non-linear delamination analysis of multilayered functionally graded circular shafts in torsion. *Journal of Applied Mechanics and Technical Physics* **59** 1104-1110.

[25] V. RIZOV (2021) Delamination analysis of multilayered beams exhibiting creep under torsion. *Coupled Systems Mechanics* **10** 317-331.

[26] N. ARUTUNIAN, B. ABRAMIAN (1963) "Torsion of elastic solids". GIFML.

[27] G. DHODT, A. CHERGUI, F.-G. BUCHHOLZ (2001) Computational fracture analysis of different specimens regarding 3D and mode coupling effects. *Enginnering Fracture Mechanics* **68** 383-401.

[28] V. RIZOV (2015) Analysis of mixed mode II/III fracture in sandwich beams. *Multidiscipline Modelling in Materials and Structures* **11** 75-87.